Bioactive Materials 6 (2021) 1479–1490

Contents lists available at ScienceDirect

Bioactive Materials

journal homepage: www.sciencedirect.com/journal/bioactive-materials

Antibacterial, pro-angiogenic and pro-osteointegrative zein-bioactive glass/copper based coatings for implantable stainless steel aimed at bone healing

Laura Ramos Rivera [a], Andrea Cochis [b,c], Sarah Biser [a], Elena Canciani [d], Sara Ferraris [e], Lia Rimondini [b,c,**], Aldo R. Boccaccini [a,*]

[a] Institute of Biomaterials, Department of Materials Science and Engineering, University of Erlangen–Nuremberg, Erlangen, Germany
[b] Department of Health Sciences, Università del Piemonte UPO, Novara, Italy
[c] Center for Translational Research on Autoimmune and Allergic Diseases–CAAD, Novara, Italy
[d] Department of Department of Biomedical, Surgical and Dental Sciences, Thin Section Lab, University of Milan, Milan, Italy
[e] Department of Applied Science and Technology, Politecnico di Torino, Turin, Italy

ARTICLE INFO

Keywords:
Zein
Bioactive glass
Copper
Bone
Antibacterial

ABSTRACT

Stainless steel implants are suitable candidates for bone replacement due to their cytocompatibility and mechanical resistance, but they suffer from lack of bioactivity and are prone to bacterial infections. Accordingly, to overcome those limitations, in this study we developed by electrophoretic deposition (EPD), an innovative surface coating made of (i) *zein*, a natural fibroblast-friendly polymer, (ii) *bioactive glass*, a pro-osteogenic inorganic material and (iii) *copper containing bioactive glass*, an antibacterial and pro-angiogenic material. FESEM images confirmed that porous, uniform and free of cracks coatings were obtained by EPD; moreover, coatings were resistant to mechanical stress as demonstrated by the tape test, resulting in a 4B classification of adhesion to the substrate. The coatings were cytocompatible as indicated by metabolism evaluation of human fibroblasts, endothelial cells and mature or progenitor osteoblasts cultivated in direct contact with the specimens. They also maintained pro-osteogenic properties towards undifferentiated progenitor cells that expressed osteogenic genes after 15 days of direct cultivation. Copper conferred antibacterial properties as biofilm formation of the joint pathogens *Staphylococcus aureus, Staphylococcus epidermidis and Escherichia coli* was significantly reduced in comparison with copper-free coatings ($p < 0.05$). Moreover, this anti-infective activity resulted as targeted towards bacteria while the cells viability was preserved when cells and bacteria were cultivated in the same environment by a co-culture assay. Finally, copper ability to recruit blood vessels and to inhibit bacterial infection was confirmed *in vivo* where the growth of *S. aureus* biofilm was inhibited and the formation of new (<50 μm diameter spread) blood vessels was observed.

1. Introduction

Osseointegration of orthopedic implants occurs through different steps starting from the primary interaction with body fluids and on-site inflammation, followed by the formation of a cell layer and the initial production of bone at the surface and its subsequently remodeling. Accordingly, in the first stage of anchorage, it is necessary to establish a strong link between the adjacent bone tissue and the surface of the implant. In addition, the placement of orthopedic implants at osseous sites in the human body, for example in fracture fixation or joint replacement, is often accompanied by a risk of bacterial contamination since a physiological milieu favorable to the metabolism of bone-related cells is also beneficial for the adhesion of microbes [1]. The result is that nowadays infections are the first reason of implant failure in orthopedics [1].

Traditional antibiotics have reduced levels of effectiveness due to the continuous evolution of bacterial resistance. In an effort to avoid bacterial attachment and surface colonization of implants, and to facilitate the integration of host tissues, the addition of biologically active materials containing antibacterial substances is gaining increasing attention

* Corresponding author. Institute of Biomaterials, Department of Materials Science and Engineering University of Erlangen–Nuremberg, Erlangen, Germany.
** Corresponding author. Department of Health Sciences Center for Translational Research on Autoimmune and Allergic Diseases–CAAD University of Piemonte Orientale UPO, Novara, Italy.
E-mail addresses: lia.rimondini@med.uniupo.it (L. Rimondini), aldo.boccaccini@ww.uni-erlangen.de (A.R. Boccaccini).

https://doi.org/10.1016/j.bioactmat.2020.11.001
Received 30 August 2020; Received in revised form 30 October 2020; Accepted 1 November 2020

[1,2]. Both natural and synthetic polymeric materials have been used extensively as platforms for the delivery of drugs, by providing a modulated load of antibacterial agents and various release characteristics, such as targeted ion release, pH change or thermoreactive capabilities [2,3]. However, it is essential to obtain a strong bonding between the nearby bone tissue and the implant surface, which can be reached by coating metal surfaces with bioactive materials such as bioactive glasses or hydroxyapatite. Bioactive glass (BG) of 45S5 composition (45.0 wt% SiO_2, 24.5 wt% Na_2O, 6.0 wt% P_2O_5, 24.5 wt% CaO), which was discovered by Hench et al. in 1971 [4], can boost the regenerative process of the organism to stimulate bone growth (osteostimulation) [4]. The osteostimulation process is associated with a gradual delivery of calcium, phosphorus and silicon ions at specific rates, resulting in a series of cellular reactions to enhance cell proliferation and growth [5]. Biopolymer and BG-based composite coatings should provide a number of extra advantages for orthopedic applications such as suppressing the potential release of harmful ions from the metallic surface, and improving the attachment and spread of musculoskeletal cells [6,7].

In order to formulate an antibacterial and pro-regenerative surface for bone implants, combinations of biologically active ions and polymers in one coating system are being increasingly investigated [8]. For this purpose, copper (Cu) is a very interesting candidate as it has been demonstrated to have an influential effect on angiogenesis [9] as well as being a strong antibacterial agent [9]. Studies have revealed the remarkable distribution of Cu in human endothelial cells when they were induced to undergo angiogenesis [10]. Another research found that copper, in combination with FGF-2 growth factor, stimulates in vitro angiogenesis [11]. It has also been demonstrated that Cu promotes the growth of human endothelial cells and leads to enhanced mesenchymal stem cell (MSC) differentiation into the bone marrow lineage [12]. The use of copper as an antibacterial material in healthcare settings has been the subject of intense interest, as many recent studies have addressed the technical aspects of the "contact killing" effect of copper [13]. It was discerned that living organisms that come into contact with copper surfaces after a prolonged incubation do not recover, since the effect of copper in contact occurs at a rate of about 7 or 8 logs per hour [14]. The direct incorporation of Cu ions into bioactive glass 45S5 was investigated by Hoppe et al. [15] with the aim of producing a Cu-doped bioactive glass and scaffolds for bone tissue engineering. Cu-doped BG was also investigated by Bari et al. [16] and Bejarano et al. [17] using the sol-gel technique to obtain mesoporous and nano-sized particles for biomedical applications, respectively. Bari et al. focused on the potential antibacterial effect of the mesoporous particles and its effectiveness in reducing biofilm formation. Similarly, Rau et al. [18] described the influence of the incorporation of Cu in the structure of BG and its effects on the formation of HA and reduction of bacterial infection.

Metallic alloys have some drawbacks beyond their advantages regarding mechanical strength and stiffness. Such disadvantages are mainly related to the potential ion release into the human body upon surface corrosion and encapsulation by fibrous tissue due to lack of bioactivity, which reduces the implant long-term stability [1]. Stainless steel 316 L can be considered a suitable material for biomedical applications displaying proper biocompatibility and some advantages in comparison with other reference metals related to mechanical properties and lower costs. However, despite these positive points, stainless steel shows some drawbacks in terms of biological integration with the surrounding tissue, which can be overcome by applying proper coatings providing pro-integrative properties [19].

Accordingly, an alternative approach with increasing popularity, which counteracts the above-mentioned problems, involves the modification of the metallic implant surface with bioactive materials in order to induce osteointegration with the host tissue. This approach combines the ideal bulk properties (tensile strength and stiffness) of the metal with the required surface properties (corrosion protection, osteoinductivity and osteoconductivity, antibacterial effects) provided by suitable coatings. In order to modify the surface of metallic implants with bioactive materials, such as BG and hydroxyapatite, electrophoretic deposition (EPD) appears to be a promising technique as it is simple, cost-effective and can produce homogeneous coatings at room temperature [20]. In fact, many deposition techniques for the surface modification of implantable biomaterials have been used to address the problem of the insufficient bioactivity of metallic implants. For instance, thermal and plasma spraying [21], magnetron sputtering [22], among others, are techniques allowing to produce bioactive coatings. However, these technologies require high energy, high temperature and/or low pressures being more cost-intensive than EPD; moreover, they prohibit the incorporation of polymeric materials as coating components, which are important for the control of the degradation of bioactive particles aimed at improving the compatibility with the surrounding tissue. In this way, EPD is a technique which allows producing coatings incorporating active molecules, e.g. natural polymers or antibiotics, at low temperature (typically room temperature). EPD first gained increasing attention in the 1980s, even though the process has been known since 1808, its first practical use occurred in 1933 [23]. Due to its high versatility when different kinds of materials are used and its cost-efficiency requiring simple equipment, EPD has established itself as a suitable coating technique for medical applications in recent years [23–25]. EPD has been shown to be the technique of choice especially for the fabrication of biopolymer coatings containing inorganic bioactive fillers, for example, combinations of chitosan, alginate and zein with bioactive glasses [26–28].

The protein zein is a unique and complex natural biopolymer; it belongs to the alcohol-soluble proteins and is the major storage of protein from corn [29]. Zein is biodegradable and bioadhesive and possesses special amino acids, such as leucine, which can regulate muscle protein metabolism and proline, which shows a positive effect regarding osteoclast functionality and activity, giving zein high potential for applications in the biomedical field [30].

Based on these premises, in this work zein composite coatings incorporating bioactive glass and copper doped BG were developed using electrophoretic deposition and further characterized, following our previous study on such coatings [28]. Degradation studies in PBS, cell viability studies using different cells, antibacterial activity, anti-infection protective efficacy and *in-vivo* studies in a mice model, were carried out to investigate for the first time the performance of the composite coatings in relevant settings, which led to the assessment of both the coating pro-regenerative and antibacterial properties.

2. Materials and methods

2.1. Materials and electrophoretic deposition of coatings

Bioactive glass (BG) particles of 45S5 composition with mean particle size 2.0 μm and 45S5 BG particles doped with 2.5 wt% CuO [15] with an average particle size of 5.0 μm were used. Zein powder (Z3625) was purchased from Sigma (Sigma-Aldrich, Germany). Stainless steel AISI 316 L (from Advent Research materials, England) was used as substrate. Glycerol (Sigma-Aldrich, Germany) and ethanol (Merk KGaA, Darmstadt, Germany) with 99% purity were used for EPD. Samples were prepared by laser cutting 0.2 mm thick stainless-steel discs of 1.25 cm diameter, which were used for the biological evaluation. Samples were then cleaned in a successive ultrasonic bath of acetone for 10 min, afterwards substrates were dried with compressed air. A mixture of ethanol (64%) and water (25%) with added glycerol (1%) was used to solubilize zein powder (10%) by stirring until it was completely dissolved. BG particles 10 g/L were added to the solution, with final suspensions being sonicated for 30 min. EPD was applied for 5 min at 10 V as optimized by the authors in a previous work [28]. The distance between the electrodes in the EPD cell (deposition and counter electrode) was fixed at 10 mm for the entire experiment. Obtained coatings are summarized in Table 1.

Table 1
Summary of developed specimens.

Specimen	Composition
Zein	Zein (100 wt%)
Zein/BG	Zein (75 wt%) + Bioactive glass (25 wt%)
Zein/CuBG	Zein (75 wt%) + Cu-doped Bioactive glass (25 wt%)

2.2. Coatings physical characterization

The morphology of the coatings was assessed by means of stereomicroscopy (M50, Leica, Wetzlar, Germany) and scanning electron microscopy (SEM, Auriga, Carl-Zeiss, Jena, Germany). For SEM observations after biological tests, the samples were dehydrated by alcohol scale treatment and surface sputtered with gold using a sputter coater (Q150T, Quorum Technologies Ltd., Darmstadt, Germany). The adhesion of the different coatings to the metallic substrate was evaluated by means of the tape test, according to the ASTM International standard D3359-97, *"Standard tests methods for measuring adhesion by tape test*". In brief, a grid of parallel cuts was prepared on the sample surface through a specific cutter, a pressure sensitive tape was subsequently applied on the surface and suddenly removed. The degree of damage induced by tape removal to the coating was evaluated by visual inspection. A semi-quantitative determination of the coating adhesion was made by comparison between the area of coating detachment observed on the sample and the tabulated values reported in the standard.

2.3. Degradation study

Samples were immersed in Phosphate-Buffered Saline (PBS, Sigma, Germany) for 1, 3, 7, 14, 21 and 28 days in plastic beakers with smooth and crack-free surfaces at 37 °C in an orbital shaker. SEM images were taken to observe the changes on the surface as a function of time in PBS.

2.4. In vitro cytocompatibility

2.4.1. Cell culture conditions

Commercial cell lines were obtained from American Type Culture Collection (ATCC, Manassas, USA) and cultivated following the manufacturer's instructions. Accordingly, fibroblasts (human, HGF, PCS-201-018), mature osteoblasts (human, U2OS, HTB-96), fetal pre-osteoblasts (human, hFOB, CRL-11372) and endothelial cells (human, EA.hy926, CRL-2922) were selected to test specimens' cytocompatibility in vitro. U2OS and ea.hy926 were grown in Dulbecco's Modified Eagle Medium (DMEM, Sigma Aldrich) 10% FBS (Gibco, Invitrogen, USA) and 1% antibiotics, HGF were cultivated in alpha-modified Eagle's minimum essential medium (α-MEM, Sigma Aldrich) 10% FBS, 1% antibiotics while for hFOB a 50:50 mix of MEM and Ham's F12 (MEM/F12, 1:1, Sigma Aldrich) 10% FBS (Invitrogen, USA), 1% antibiotics and 3 mg/ml neomycin (G418, Sigma) was used. All cells were grown until a 90% confluence and then collected by enzymatic digestion (trypsin/EDTA) prior to each assay. Moreover, in order to preserve the original primary phenotype, HGF and hFOB were applied until passage 10.

2.5. Direct cytocompatibility evaluation

Prior to initiating biological evaluations, specimens were heat sterilized (2 h, 130 °C in a dry oven) and afterwards moved into a sterile 12 multiwell plate. Cells were directly cultivated onto the specimens' surface in a defined number (2×10^4 cells/sample); cells were dropwise (200 μl/each) seeded directly onto the specimens' surfaces and allowed to adhere 4 h in the incubator. Then, each well was rinsed with 2 ml of fresh medium and plates were incubated for 24, 48 and 72 h. At each time-point, cells' viability was determined by means of the metabolic colorimetric Alamar blue assay (AlamarBlue®, ready-to-use solution, Thermo Fisher, Milan, Italy). Briefly, the colorimetric solution was used to replace the culture medium and allowed to react for 4 h in direct contact with cells; then, metabolized Alamar fluorescent signal was detected by spectrophotometer (Tecan, Spark, Switzerland) at 590 nm wavelength. Alamar solution was used as a background reference signal to normalize results; results were expressed as means of relative fluorescent units (RFU).

To exclude cells' membrane damage due to the coatings' composition, the release of the cytosolic enzyme lactate dehydrogenase (LDH) was measured in the supernatant after 72 h of direct cultivation. Briefly, the spontaneous LDH release was measured by mixing 50 μl of cells supernatant with 50 μl of the reagent stock solution provided by the kit (CyQUANT™ LDH Cytotoxicity Assay, from Invitrogen, ThermoFisher Scientific); after 10 min incubation, the reaction was stopped by the stop solution and fluorescence was measured by means of an spectrophotometer (Tecan, Spark, Switzerland) using an excitation of 560 nm and emission of 590 nm. Pure medium was measured as well and values were subtracted to the test values as blank; zein was considered as control. Finally, after 72 h of cultivation cell morphology was observed by SEM.

2.6. Antibacterial evaluation

2.6.1. Bacteria growth conditions

Pathogens were commercially obtained from ATCC and the manufacturer certified for their drug-resistance as well as for their ability to form a biofilm. Accordingly, *Escherichia coli* (EC, ATCC 25922), *Staphylococcus aureus* (SA, ATCC 43300), *Staphylococcus epidermidis* (SE, ATCC 14990) were chosen as target strains due to their high incidence in patients experiencing joint infections. Following the manufacturer's instructions, EC was cultivated in Luria Bertani agar medium (LB, Sigma) while SA and SE were cultivated in selective blood agar medium (Sigma). Plates were incubated at 37 °C for 24–48 h until single defined colonies were observed onto the agar surface. Then, fresh broth-cultures were prepared prior to each experiment by collecting 4–5 colonies from the agar and spotting them into 20 ml of the strain-selective medium. To perform antibacterial experiments, the obtained sub-cultures were incubated at 37 °C in agitation (120 rpm) overnight to reach the logarithmic growth phase and then they were diluted to a final 1×10^5 cells/ml high-density concentration by spectrophotometer (corresponding to an optical density = 0.001 at 600 nm).

2.7. Biofilm formation

Heat-sterilized specimens were located into a 12 multiwell plate and directly infected with 1 ml of the bacteria suspension prepared as prior described in paragraph 2.5.1. Surface biofilm formation was obtained in static conditions, as previously described [31]. Briefly, the separation between floating planktonic bacteria and biofilm-adherent ones were forced by a first agitation step using an orbital shaker (90 min, 120 rpm, 37 °C); afterwards, each media including planktonic bacteria were discharged and replaced with fresh medium to support the growth of surface-adherent biofilm. Specimens' infection was induced for 1, 2 and 3 days; at each time point, the viability of the biofilm bacteria community was determined by the alamar blue assay, as detailed in paragraph 2.4.2. Besides bacteria metabolic activity, biofilm morphology was visually checked by SEM imaging.

2.8. Cells-bacteria co-cultures

2.8.1. Specimens infection

To verify the coating ability to protect cells undergoing healing from bacterial infection, a co-culture assay was applied as previously shown by the authors [32]. Osteoblast progenitors hFOB were selected as cells deputed for tissue healing and seeded onto the specimens' surface at a known density (2×10^4 cells/specimen) in 1 ml of medium for 24 h to allow adhesion and spread. Then, the standard medium was replaced with an antibiotic-free medium, containing 1×10^5 bacteria (EC or SA or

SE) and specimens were incubated for 48 h in the incubator to allow cells and bacteria to compete for the same surface.

2.9. Cell and bacteria count

After 48 h incubation, samples were collected, washed with PBS to remove non-adherent cells and incubated 10–15 min with 1 ml of a collagenase (1 mg/ml) and trypsin (0.25%). After detachment, the supernatant was collected, and viable cells and bacteria counted. Cells were counted by means of Bürker chamber (using trypan blue to distinguish viable cells) while the bacteria number was evaluated by colony forming unit (CFU) count onto LB agar plates, as previously detailed by Ferraris et al. [33].

2.10. Osteogenic properties

To verify the coatings' ability to support osteogenesis, progenitor hFOB cells were seeded onto the specimens' surface at a known density (1×10^4 cells/specimen) and allowed to adhere for 24 h in an incubator; then, cells were cultivated in the presence of osteogenic medium (DMEM 10% FBS supplemented with 50 nM dexamethasone, 0.2 mM ascorbic acid, and 10 mM b-glycerophosphate, all from Sigma) for 15 days. The medium was refreshed every 3 days, collected and used to evaluate alkaline phosphatase (ALP) activity in the supernatant by means of a colorimetric assay (ab83369, from AbCam, UK). Finally, the expression of osteogenic genes collagen I (COL 1), ALP and osteopontin (OPN) was evaluated after 15 days by real-time PCR to confirm cell differentiation into bone-like lineage. Briefly, cells were homogenized in TRIzol reagent (Sigma) and RNA isolated by isopropanol precipitation; cDNA was obtained by RNA reverse transcription using a TaqMan kit (from Applied Biosystems, USA). For real time PCR TaqMan Gene Expression Assays (Applied Biosystems) were used on a GeneAmp 7500 Real Time PCR System (Applied Biosystems) using 18S rRNA (Applied Biosystems 4310893E) as housekeeping gene. Finally, the expression level of the selected osteogenic genes after 15 days into differentiative medium was normalized towards the starting expression level (intended as the seeding day expression) by the $^{\Delta\Delta}$Ct calculation.

2.11. In vivo antibacterial and pro-angiogenic properties

2.11.1. Animals

All the surgical procedures described below were previously fully approved and authorized by the University of Piemonte Orientale ethical committee and by the Italian Ministry of Health (official authorization protocol n. 854/2017-PR). Animals were fully anaesthetized during procedures (3% isoflurane by oral inhalation). 16 weeks-old adult wild type mice (C57BL/6JOlaHsd, purchased from Envigo, Italy) were used for the experiment. Animals were hosted in the animal enclosure of the University of Piemonte Orientale following a 12 + 12 h dark/light cycle with a 25 °C ambient temperature, administrated with diet food (provided by Harlan, Udine, Italy) and bi-distilled water (from Millipore).

2.12. Subcutaneous implantation

Animals were fully anaesthetized during procedures (3% isoflurane general anesthesia by oral inhalation). Samples were implanted into a skin pocket in the mice dorsal skin, as previously described [34]. Briefly, a 1 cm skin excision was done by sterile surgical forceps to introduce the specimen into the pocket; then, 4.0 VICRYL® sutures (polyglactin 910, Ethicon, USA) were used to close the wound. Animals undergoing surgeries were administrated with general analgesia (0.15 mg/10 g flumequine + 0.15 mg/10 g sodium metamizole) by subcutaneous injection. Finally, animals were anaesthetized and euthanized by carbon dioxide inhalation.

2.12.1. In vivo anti-infective properties evaluation

To test copper ability to preserve implants' surface integrity from bacterial infection, specimens were pre-infected with 1×10^3 *S. aureus* bacteria/scaffold and then introduced *in vivo* in the mice subcutis pocket to grow the bacteria into a nutrients-rich environment. Surgical implantation was performed as prior detailed in paragraph 2.8.2 and maintained for 7 days. After animals sacrifice, specimens were extracted from the pockets and carefully cleaned up from tissues; finally, the number of viable bacteria that had survived onto the specimens' surface was counted with the CFU method after bacteria detachment by vortex and sonicator (3 times, 30 s each).

2.12.2. Tissue ingrowth and blood vessels recruitment

Six specimens were subcutaneously implanted as prior described (1 specimen/mice). After 1 month they were collected and analyzed to investigate under optical microscope the interface between the disk and subcutaneous tissue, the presence of inflammatory infiltrated tissue and of blood vessels in the surrounding area. For all specimens, cross-sections were prepared, allowing the analysis of the tissue in close contact with the disk surface. In brief, after fixation with 10% formalin, specimens were dehydrated by increasing the alcohols' scale, infiltrated and embedded in resin (Tecnovit 7200, Kulzer); the disks were sliced in the middle (along the diameter) and the surface mechanically polished to a final thickness of 80 μm. Histology was performed using the central slices by applying the Toluidine blue, a basic and acidophil staining which marks in blue the nuclei of the cells and all acid components of the extracellular matrix. All slides were acquired using an optical digital scanner at total magnification of 400× and a total digital magnification of 800x (NanoZoomer S60, Hamamatsu) and qualitatively and semi-quantitatively analyzed using a dedicated software NDP.view2. Blood vessels were counted in the 50 μm thin tissue layer (TL) surrounding the disk using a digital test point grid on 400x images. The blood vessels counted were expressed as percentage of total test points. Finally, the diameter of 20 blood vessels randomly observed around the implant surface was quantified to verify whether they could be considered as newly formed.

2.13. Statistics

Experiments were performed using 12 replicates/assay. Results were statistically analyzed using the SPSS software (v.20.0, IBM, USA). First, data normal distribution and homogeneity of variance were confirmed by the Shapiro-Wilk's and the Levene's test, respectively; then, groups were compared by the one-way ANOVA using the Tukey's test as post-*hoc* analysis. Significant differences were established at $p < 0.05$.

3. Results and discussion

3.1. Coatings physical evaluation

Electrophoretic coatings obtained when using a voltage of 10 V and a deposition time of 5 min are shown in Fig. 1. As can be observed, coatings produced with 10 V and a 5 min deposition time were porous, fairly uniform and free of cracks even if exhibiting different surface morphology. It can be identified that zein and zein/CuBG coatings present pores which are interconnected and have a distribution over the whole coating structure. The porosity seems to be formed by water hydrolysis and considering that zein molecules can trap bubbles that move from the bottom to the surface of the electrode during the deposition process [35]. This effect leads to the formation of holes when water inside the coating evaporates (as well as glycerol) and a porous structure is formed. The presence of CuBG particles could not be detected in the SEM images. This suggests that particles are embedded in the biopolymer matrix through the thickness of the coating. Another reason for this porous structure could be that it is induced by spaces in-between CuBG particles. In the case of zein/BG coatings it can be observed that

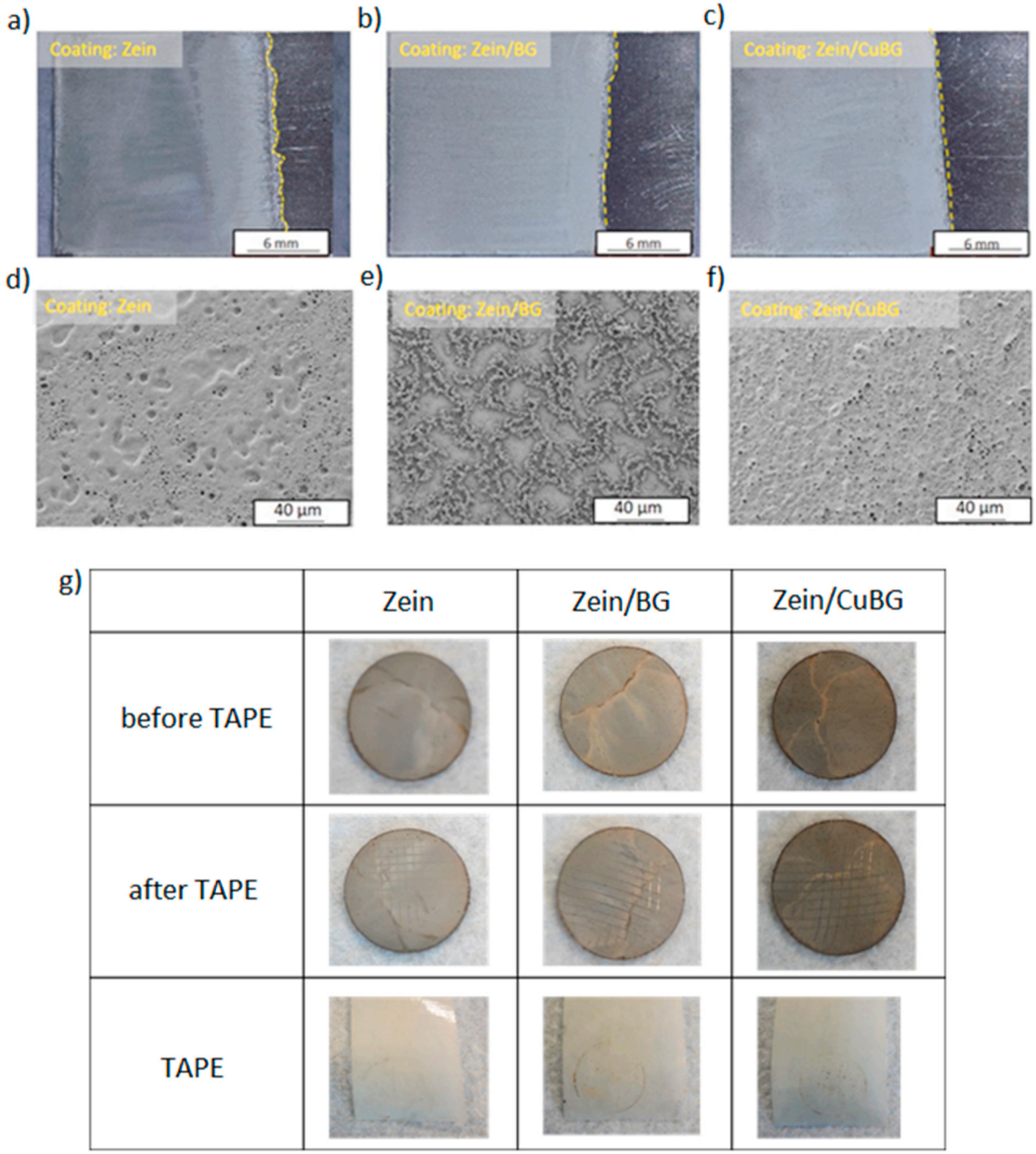

Fig. 1. Optical microscopy images of coated electrodes (upper panel) and SEM micrographs (lower panel) of zein (a, d), zein/BG (b, e) and zein/CuBG (c, f) coatings obtained by EPD at 10 V and 5 min deposition time. Results of the tape test (g) showing visual appearance of the surface before the test (first row), after the test (second row), and the tape after its removal (third row).

the "first layer" of the surface shows some zein microspheres and porosity that seems to have formed by water hydrolysis. The dendritic structure appears to be connected and formed by zein in different shapes, namely elongated tubes and microspheres [36]. BG particles were not detected by direct visual inspection. The formation of this structure can be created in two different steps. First, zein molecules that surround the electrode are deposited and form the first layer. This process is followed by the bond of BG particles with zein molecules that can lead to different shapes. It is then possible that BG particles were embedded in this worm-like structures covered by zein. The different morphologies highlighted by the SEM images can be probably attributed to the technique itself; in fact, it is possible that the movement of the particles towards the electrode differs due to their different weight and size, which influences the final surface topography of the coatings.

Finally, the tape test assay was performed in order to evaluate the coatings' resistance to mechanical stresses. Results (Fig. 1g) showed that all surfaces exhibited only limited damage after tape removal, with damaged areas mainly located at the intersections between the parallel cuts. As a confirmation, only few signs of damage are visible on the tape (with the exception of the circular mark of the disk contour). Considering these observations, coating adhesion can be classified as 4B ("small flakes of the coating are detached at the intersections. Less than 5% of the area is affected") according to ASTM 3359.

3.2. Degradation

The samples were incubated in physiological conditions using PBS from 1 up to 28 days; afterwards, they were morphologically

characterized. PBS was chosen for this test based on the ASTM-F1635 standard for the "in vitro degradation of Hydrolytically Degradable Polymer Resins and Fabricated Forms for Surgical Implants" considering that this medium possesses an ion concentration in the physiological range for the intended application. Analysing the micrographs shown in Fig. 2, in all samples, it is possible to visualize the increment of surface erosion after 3 days of immersion in PBS even if a precise evaluation of mass loss was not performed: an increase in the size of the holes and the presence of new pores are visible. This behaviour may be due to the hydration and hydrolysis occurring on the surface at the beginning of the degradation process [28]. The breakage of amide bonds is relatively fast in comparison to the diffusion rate of water into the bulk of the coating, which means that such degradation reactions are limited to the surface. This erosion can also be caused by new morphological arrangements of chain fragments [37]. For zein/BG and zein/CuBG another possibility for the surface erosion might be the changes in the local pH close to the surface. The pH likely becomes more acidic over time due to the presence of more glutamic acid molecules. This pH changes can also influence the degradability as can be observed after 28 days of immersion. During this stage, it is possible that BG and CuBG particles start to leach. Dissolution of glass particles involves a change of pH [15]. This pH change and high reactivity of the ions present in the solution can initiate the degradation of zein molecules [37]. It is possible that some of the amide groups that are removed from zein can bond with the hydroxyl groups, creating a neutral overall pH. Therefore, in the present composite coatings, the surface showed a higher biological erosion (compared with pure zein coatings) by increasing the immersion time. This behaviour of surface eroding is desirable since it would lead to a possible release of ions from the glass particles through the porous surface facilitating interaction with the physiological fluids to form HA (the typical effect provided by BGs [38]) and enabling the release of copper ions, one of the functionalities of the present coating system.

3.3. In vitro cytocompatibility

Copper has been shown to be an ion that is involved in various functions in the body such as the regulation of factors for the expression of VEGF, however, in high amounts, it can be toxic and promote the progression and severity of different illness [39]. Indeed, ionic dissolution products of this type of CuBG were shown at therapeutic dose to reduce apoptosis of HUVEC cells as well as increase factor expression in keratinocytes [15,40]. In fact, the present results demonstrated that the insertion of BG (zein/BG) or CuBG (zein/CuBG) did not lead to a reduction of cell viability in comparison with pure zein that, was considered as control (Fig. 3, $p > 0.05$), due to the comparable results obtained in relation to polystyrene (displayed in the Supplementary Fig. 1). Accordingly, the viability of osteoblast progenitors hFOB (Fig. 3a), mature osteoblasts U2OS (Fig. 3b), primary HFG fibroblasts (Fig. 3c) and human endothelial cells EA.hy926 (Fig. 3d) was not reduced in the presence of copper (zein/CuBG) in comparison with pure zein. Finally, SEM images (Fig. 3e) further demonstrated that cells were able to adhere and spread onto zein/CuBG coatings thus confirming the cytocompatibility of the applied coating to all possible cell lineages potentially in contact with the implant in physiological conditions.

The use of zein as the organic component of the composite coatings contributes to the control of the degradation and brittleness of the BG particles, and enhances the adhesion to the substrate without the need of additional treatments. Furthermore, zein helped to stabilize glass particles in aqueous suspensions enabling EPD of composite coatings and homogeneous and fairly uniform coatings were obtained. Moreover, when immersed in SBF, zein can control the mineralization of the Ca/P layer as shown in our previous study [28], and eventually leads to an improved in vitro cellular response. In fact, the coatings were demonstrated to maintain their bioactivity as an HA layer was observed after 21 days of SBF immersion (results previously shown in Ref. [28]). From the point of view of the present study, regarding the beneficial impact of composite coatings without requiring the use of additional biological factors, it is of great value to consider the potential of zein as an entity to enhance surface performance such as mineralization, cell adhesion and proliferation.

After the assessment of the cells' metabolic activity by alamar blue, LDH release was measured into the supernatant to evaluate the release of the cytosolic enzyme lactate dehydrogenase due to a possible plasma membrane damage. The evaluation was done after 72 h, the longest time-point selected for the cytocompatibility in order to compare results with alamar blue data. Zein/BG and zein/CuBG results were compared with the pure zein data as such coatings reported similar value to polystyrene (gold standard) (detailed in the Supplementary Fig. 2). As reported in Table 2, the quantification of LDH released in the medium after 72 h of direct contact between cells and coatings revealed that no significant differences were appreciable by comparing test (zein/BG and zein/CuBG) and control specimens ($p > 0.05$). Thus, LDH values

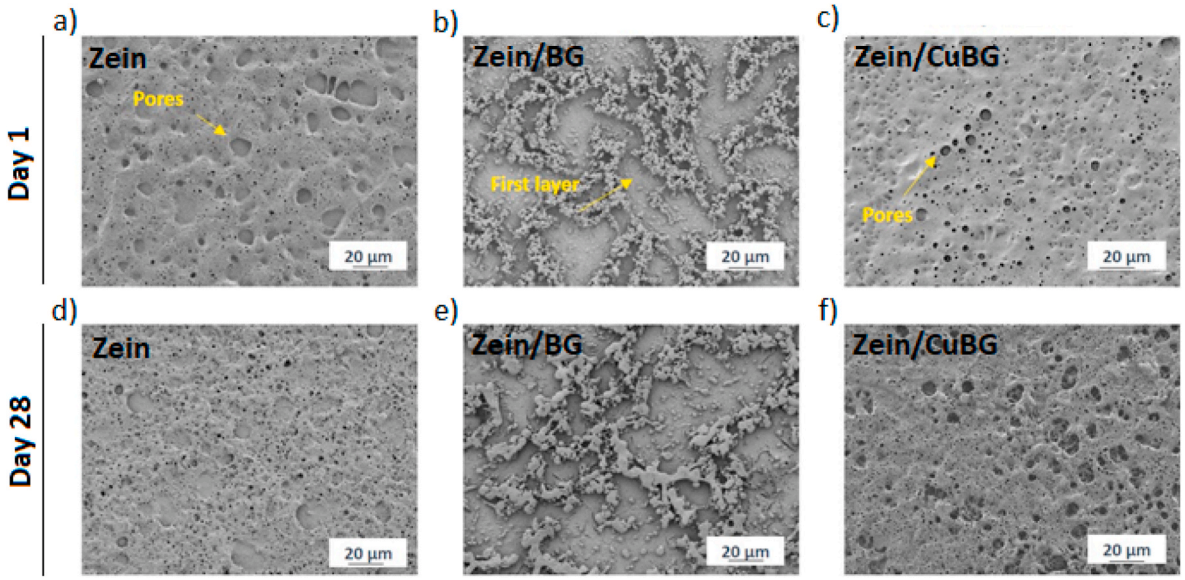

Fig. 2. SEM micrographs of zein (a, d), zein/BG (b, e) and zein/CuBG (c, f) after 1 (upper panel) and 28 (lower panel) days of degradation, showing the change of coating surface morphology.

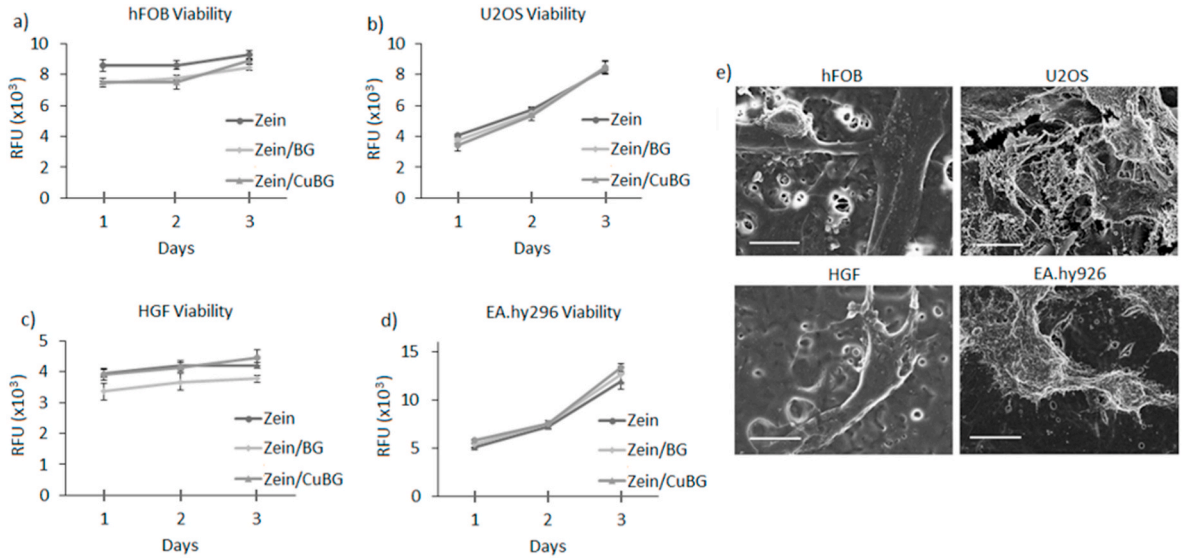

Fig. 3. Coating cytocompatibility. No significant differences were noticed between zein and zein/BG or zein/CuBG coatings for all the tested cells (a-d, $p > 0.05$). SEM images (d) representative of zein/CuBG at day 3 confirmed that cells adhered and spread. Scale bar = 10 μm.

Table 2
Spontaneous LDH release in the medium: quantification after 72 h of direct cultivation. Results are expressed as Relative Fluorescent Units (RFU). Results are expressed as means ± standard deviations.

Cells	LDH release (RFU – 72 hs)		
	Zein (cnt)	Zein/BG	Zein/CuBG
hFOB	168 (±11)	178 (±14)	182 (±22)
U2OS	111 (±5)	116 (±8)	129 (±18)
HGF	180 (±16)	186 (±11)	195 (±21)
EA.hy296	155 (±9)	167 (±13)	172 (±16)

indicated the absence of toxicity exerted by the coatings confirming the results obtained by the metabolic activity assay alamar blue.

3.4. Antibacterial activity

The results concerning antibacterial activity by contaminating the coatings directly in contact with *S. aureus* (Fig. 4a), *E. coli* (Fig. 4b) and *S. epidermidis* (Fig. 4c), respectively, are reported in Fig. 4. Zein was considered as control assuming that the highest number of bacteria adhered onto such surface after the biofilm-planktonic separation phase due to the lack of antibacterial properties. As expected, zein and zein/BG coatings did not show a decrease in the bacteria metabolism at each tested time point. On the other hand, the introduction of copper (zein/CuBG) resulted in a sharp reduction in the viability of adhered bacteria cells in comparison with zein and zein/BG coatings. Results obtained with *S. aureus* (Fig. 4a) confirmed copper efficacy. Even if the effect was less marked at 24 h, a decrease in biofilm viability was observed in the following days. For *S. epidermidis* biofilm, the effect was less evident (Fig. 4c). Here, differently to what was obtained for *E. coli* and *S. aureus*, only a small reduction in terms of biofilm viability was observed after 24 h. Moreover, no marked biofilm reduction was observed in the following days, thus suggesting a certain strain resistance even in a continuous treatment. However, FESEM images showed differences of biofilm aggregates formation, as in the copper doped surface the presence of dense clusters appeared to be reduced in comparison to zein/BG coatings. In detail, *E. coli* (Fig. 4b) displayed similar results for zein and

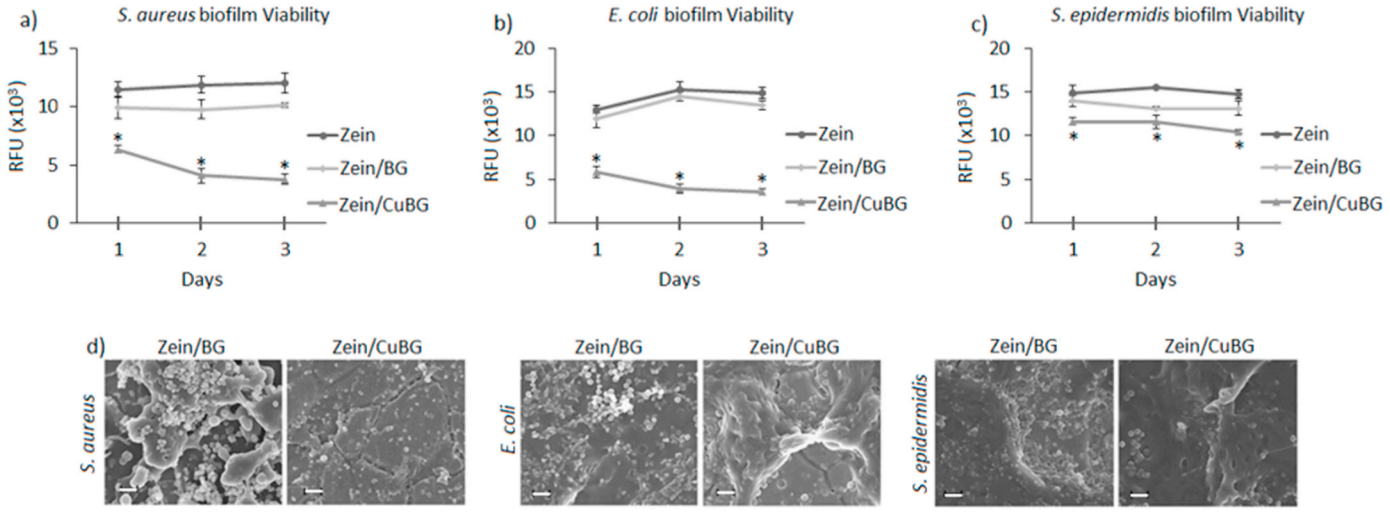

Fig. 4. Antibacterial activity results. The introduction of copper into bioactive glass (zein/CuBG) determined a significant reduction of bacteria viability in comparison with both zein and zein/BG (a-b-c, $p < 0.05$, indicated by *). (d) SEM images showing the lack of evident biofilm aggregates on zein/CuBG coatings. Scale bar = 10 μm.

zein/BG; although when copper was introduced, a marked reduction in terms of biofilm viability was detected after 24 h. Moreover, after 48 and 78 h the thickness of biofilm decreased thus suggesting that the release of Cu ions continues over time inhibiting biofilm formation. Finally, representative SEM images for 72 h biofilm confirmed the lack of biofilm biomass on the zein/CuBG surfaces (Fig. 4d).

As mentioned previously, copper is involved and regulates different metabolic activities of many enzymes such as tyrosine, dopamine among others, since they require copper as a donor/receptor. However, the amount of copper must be regulated to obtain the highest advantage of its antibacterial capability without the negative influence (toxicity) on the cell metabolism [41,42]. Depending on the copper coordination, reactive hydroxyl radicals can be introduced in a Fenton-type reaction, leading to a series of disadvantageous interactions with cellular molecules, such as the oxidation of proteins and lipids [42].

3.5. Co-cultures

To verify whether the copper-doped bioactive glass was able to protect cells from a secondary infection, a co-culture assay was performed. To evaluate cells and bacteria behaviour under the same conditions as for surface colonization, a co-culture assay was designed, enabling the confirmation of copper targeted activity towards bacteria while preserving cells' metabolism. Results showing the anti-infection protective efficacy of the coatings are reported in Fig. 5. As shown, the initial number of seeded cells (2×10^4/specimen) was found to increase when specimens were infected with *E. coli* and *S. aureus* (Fig. 5a and b) or at least preserved if the infection was induced with *S. epidermidis* (Fig. 5c). This was a confirmation that samples containing CuBG favored cell adhesion and spreading, displaying a protection function in respect to bacteria colonization. In accordance with this result, the initial number of bacteria (1×10^5 cells/ml) was decreased by the presence of copper, as shown in Table 3. Considering the values obtained by zein and zein/BG, the number of bacteria was reduced by about 6–7 logs by coatings containing copper for *E. coli* and *S. aureus*; and, as expected from previous results, a small inhibition was obtained for *S. epidermidis*, where a reduction of about 3 logs was measured in comparison with zein and zein/BG. Considering instead the initial number of bacteria, it should be noticed that it was reduced by about 1–3 logs by the presence of copper; therefore, a partial number of bacteria was able to colonize the surface of the zein/CuBG coatings. These results suggest that the release of copper ions successfully protected the coating from biofilm formation and provided a selective activity towards bacteria. Finally, SEM micrographs (Fig. 5d, representative for hFOB - *S. aureus* infection) show the biofilm formed on samples containing bioactive glass (indicated by the yellow square) in which the shape of apoptotic cells is observed due to the infection raise (indicated by the yellow arrows). On the other hand, samples containing CuBG show that a significant number of cells adhered and spread, indicating the protection function of the coating limiting bacteria colonization. In particular, SEM images failed to show the presence of evident biofilm-like bacteria aggregates onto copper-doped BG containing coatings, thus confirming that adhered bacteria colonized the specimens' surface mostly as random single colonies.

Table 3
CFU count of co-cultures assay for the different coatings and bacteria investigated (* = $p < 0.05$ vs zein control).

Specimen	*S. aureus* CFU	*E. coli* CFU	S. epidermidis CFU
Zein	8,33E+09	1,60E+09	5,33E+07
Zein/BG	1,27E+09	5,00E+08	1,30E+07
Zein/CuBG	2,40E+03*	5,67E+02*	3,00E+04*

3.6. Osteogenesis

After verifying the coatings' ability to support cell proliferation and to inhibit bacterial infection, the possibility to induce osteogenesis was investigated. In the coating formulation hypothesis, the use of bioactive glass was aimed to this purpose as it is well known that BGs represent one of the most interesting inorganic materials favoring the formation of bone-like matrix due to their chemical composition and intrinsic bioactivity [43,44]. In fact, in general when BGs are introduced into a physiological environment, Na^+ and Ca^{2+} ions are released and a hydrated silica gel forms on the surface. Hydroxycarbonate apatite (HCA) then crystalizes on the surface through constant incorporation of Ca^{2+}, PO_4^{3-}, OH^-, and CO_3^{2-} [45]. In this study, osteogenesis was investigated from the biological point of view once hFOB cells were cultivated on the surfaces. Results are reported in Fig. 6. As expected, the presence of BG (zein/BG and zein/CuBG coatings) speeded up cell differentiation in comparison to the pure zein coating; ALP release in the medium (Fig. 6a) after 7 and 10 days for both zein/BG and zein/CuBG coatings was

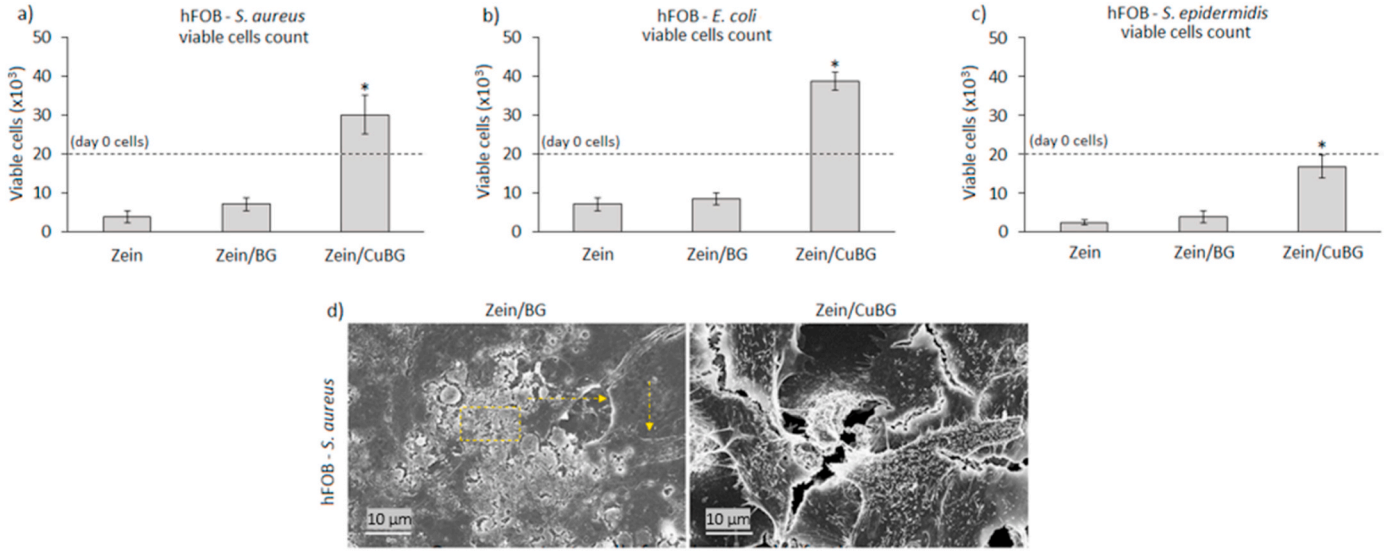

Fig. 5. hFOB-bacteria co-cultures. Only zein/CuBG coatings were able to preserve the initial number of cells (a-c, 2×10^4, starting number indicated by the dashed lines); results were significant for all the tested strains (a-c, zein/CuBG vs zein or zein/BG, $p < 0.05$, indicated by *). Representative SEM images (d) of hFOB-aureus culture showing high biofilm contamination for zein/BG but normal cells for zein/CuBG coatings.

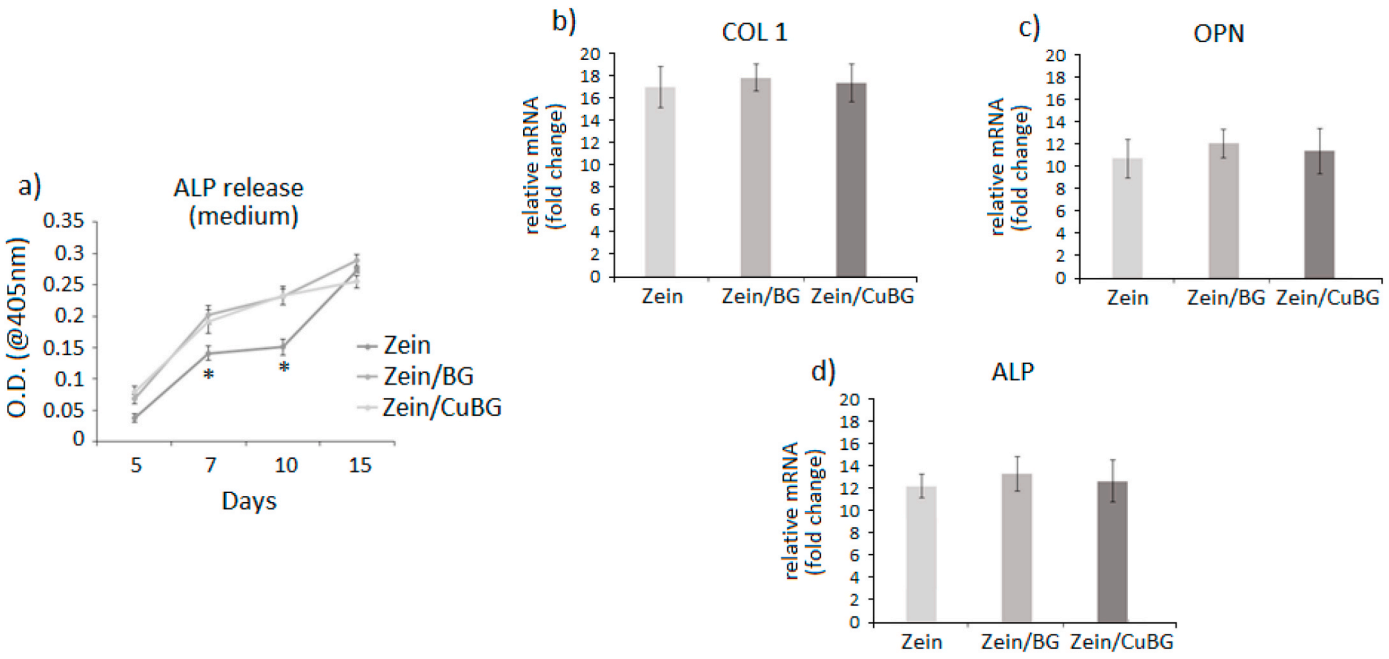

Fig. 6. Osteogenesis results. The presence of bioactive glass (zein/BG and zein/CuBG) improved the release of ALP at day 7 and 10, in comparison with zein coatings (a, $p < 0.05$, indicated by *). After 21 days osteogenic genes collagen I (COL 1, b), osteopontin (OPN, c) and alkaline phosphatase (ALP, d) were similarly expressed for all the tested coatings, suggesting a similar cell maturation.

significantly higher in comparison with that for pure zein coatings ($p < 0.05$, indicated by *) thus confirming the BG pro-osteogenic stimulation. However, also zein alone was successful in supporting osteogenesis as after 15 days all values were comparable, suggesting similar cell maturation. As a confirmation, gene expression representative after 15 days cell culturing revealed that cells seeded onto all tested coatings expressed similar levels of osteogenic genes collagen I (COL 1, Fig. 6b), osteopontin (OPN, Fig. 6c) and alkaline phosphatase (ALP, Fig. 6d). The lack of significant differences in osteogenic gene expression suggests that copper in the used concentration range did not interfere with stem cells differentiation. This is an important finding as previous work had suggested that released metallic ions can be a negative factor for cell differentiation [46]. For example, Xie et al. recently demonstrated how an excessive uptake of silver could strongly affect cells' fate by lowering osteogenesis (downregulation of collagen I, ALP, osteocalcin and osteoprotegerin) and favouring osteoclast-like expression of Runx2 and RANKL, thus leading to a possible impairment of the bone remodeling process [47].

3.7. *In vivo results*

3.7.1. *Antibacterial activity*

Specimens were pre-infected and implanted subcutaneously in mice to test whether the efficacy was confirmed in a physiological nutrients-rich environment following a pre-validated model for antibacterial coatings evaluation [48]. *S. aureus* was selected as test strain and the starting inoculum (1×10^3 bacteria) was applied as sufficient to determine severe joint infection [48]. Accordingly, after 1-week implantation, specimens were collected and the CFU number of bacteria grown on the coating was counted. Zein coating was considered as control group in continuity with the in vitro experiments and for comparison with the zein/BG and zein/CuBG test groups. Results are reported in Fig. 7b. Interestingly, while in copper-free zein control and in zein/BG specimens the number of CFU was basically in the same ratio of the starting inoculum (10^3), in the coating doped with CuBG no viable colonies were counted even if it must be taken into account that a certain number of bacteria can be lost due to the removal procedures. This implies that, while in mice carrying zein and zein/BG coatings the infection was not reduced, in the zein/CuBG ones the induced infection was stopped. The employment of a wild type mice suggests that the immune system may have had an active role in counteracting the infection; however, the differences noticed between control (zein) and test groups (zein/BG and zein/CuBG) suggest at the same time that copper was a key factor in eradicating the infection.

3.7.2. *Tissue ingrowth and angiogenesis*

Besides its antibacterial potency, copper was here selected also for its known pro-angiogenic role, as discussed above [49,50]. Results obtained in terms of cytocompatibility using human endothelial cells (EA. hy962, Fig. 3d) were not satisfactory from this point of view, as no stimulation in terms of metabolic activity was observed for zein/CuBG coatings in comparison with zein and zein/BG. The pro-angiogenic copper role was then re-evaluated *in vivo* in terms of the ability of the coating to recruit blood vessels at the implant site. Results are reported in Fig. 7e-l.

First, the formation of new tissue around the implants was evaluated. The ground sections showed that the subcutaneous tissue was in contact with the coatings for all zein (c-*d*-e), zein/BG (f-g-h) and zein/CuBG (i-j-k) samples without alteration of the healing process. No signs of tissue and cell reactions were observed, in particular, no inflammatory infiltrate and necrosis were detected. At higher magnification and setting the digital camera with an exposure time of 1/300 s (e-h-k), it was possible to observe in the shadow of the implant the presence of about 50 μm thin tissue layer (TL) in close-contact with the coatings. The TL was characterized by the presence of fibroblast-like cells surrounded by collagen fibers that ran parallel to the coating. In the TL blood vessels were distributed in different manner in the three coatings. In zein few vessels were visualized (Fig. 7d) while no vessels were observed for zein/BG (Fig. 7g); on the opposite, when cooper was included (Fig. 7j) a proportion of approximately 17.5% ± 8% blood vessels was counted.

The lack of vascularized tissue on zein/BG coatings suggests that the topography of the coating plays a role in the angiogenic behaviour. Since zein and zein/CuBG coatings showed a highly porous surface, it can be suggested that on such coatings, cells can create more connections. It

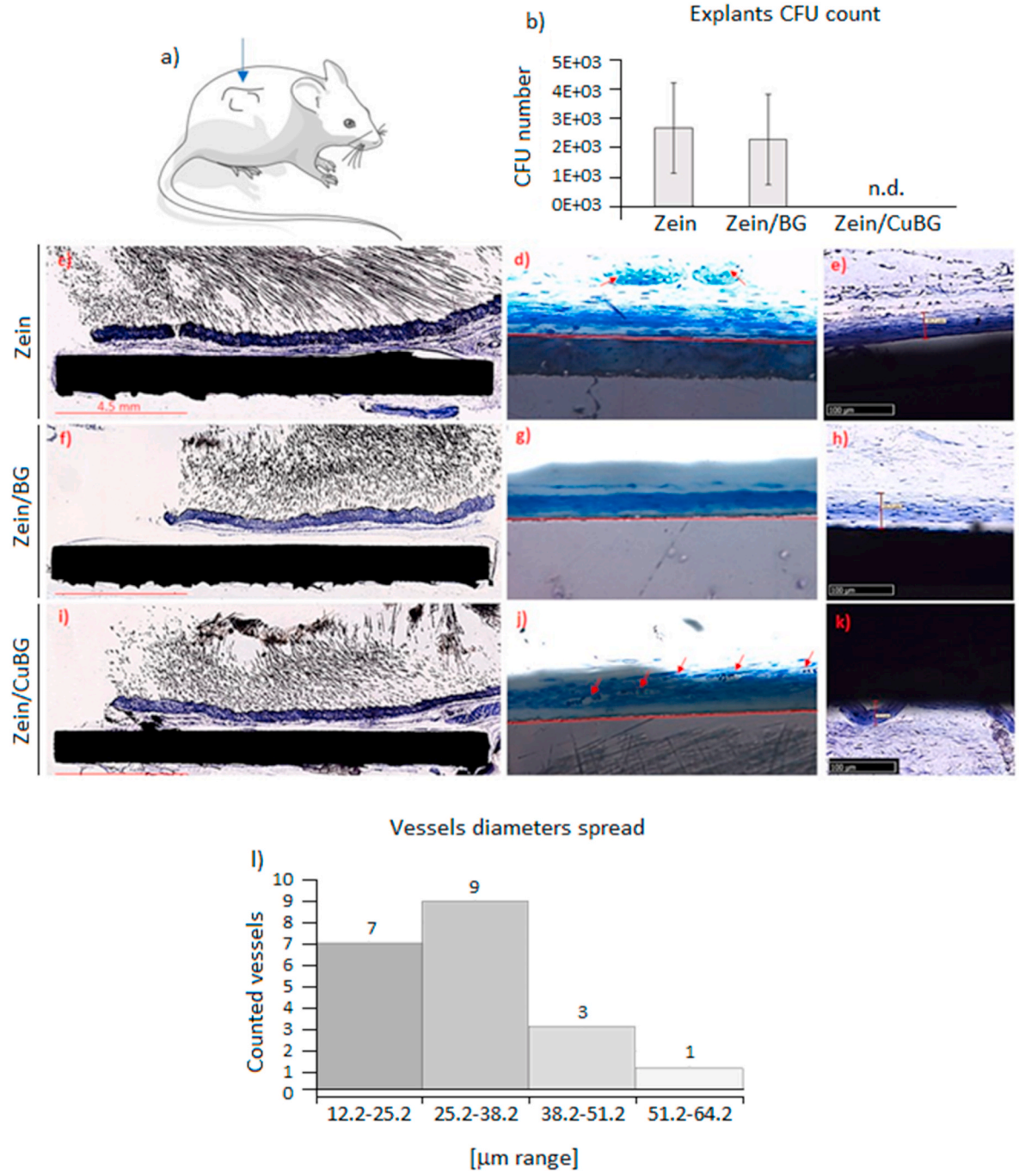

Fig. 7. In vivo results. In the subcutaneous implant model (a), copper addition (zein/CuBG) caused the inhibition of the induced infection (b) in comparison with zein (control) and zein/BG. All zein (c-*d*-e), zein/BG (f-g-h) and zein/CuBG (i-j-k) coatings supported similar tissue thickness formation of about 50–55 μm. Vessels count (d-g-j) confirmed that zein/CuBG coatings recruited the highest number of vessels (indicated by red arrows) that were verified as newly formed (<50 μm) by the diameter spread evaluation (l). (For interpretation of the references to color in this figure legend, the reader is referred to the Web version of this article.)

also seems that for zein/BG thinner tissue was formed whereas almost no blood vessels were detected. In zein/CuBG coating, the vessels diameter presented a range between 12 μm (range 12.2–25.2) and 55 μm (range 51.2–64.2). Fig. 7l details that about 80% of the vessels evaluated were included in the range 12.2–38.2 μm and that 95% was <50 μm. Accordingly, results suggest that copper ions have stimulated the formation of blood vessels in the early stage, which resulted in the formation of a larger number of lumens of smaller radius (<50 μm) surrounded by a thin wall.

These findings do not represent a novelty giving however a confirmation to the initial hypothesis related to the Cu ability to act as a chemoattractant for blood vessels. In fact, copper activity in favoring angiogenesis can be attributed to the activation of HIF-1α leading to the upregulation of vascular endothelial growth factor (VEGF) [51]. VEGF plays a pivotal role in angiogenesis by regulating endothelial cell proliferation and migration; interesting, VEGF expression is promoted if the microenvironment results as hypoxic. The presence of copper was demonstrated to influence the stability of the oxygen sensor protein HIF-1α in hypoxia; in such conditions, VEGF and other pro-angiogenic genes are activated by the presence of HIF-1α thus initiating the neovascularization process [51]. Therefore, by the subcutis *in vivo* model, copper antibacterial and pro-angiogenic properties were shown. Such

model can be considered as appropriate for such evaluation as the formation of blood vessels was due to soft tissue in touch with the specimens as well as the presence of bacteria seeded directly onto the specimens' surface, thus simulating possible pathogen surface colonization after the surgical procedure [48]. However, it must be highlighted that by this model no information about specimen-guided bone healing was provided as these data can be achieved only by a direct implant into an injured site. This, from this point of view, more studies are required to confirm zein/CuBG suitability as bioactive coating for bone implants.

4. Conclusions

Zein and zein/BG or zein/CuBG coatings were successfully applied onto stainless steel substrates by the EPD method confirming the suitability of such treatment to introduce bioactive elements on metallic surfaces. The coatings were resistant to mechanical solicitations as well as they visually appeared as poorly degraded after long time immersion in physiological conditions. The presence of BG and antibacterial Cu conferred osteoconductive and anti-infective properties to the bulk material, thus overcoming the poor bioactivity of the metal. In particular, the addition of copper to the bioactive glass coupled with zein was successful in significantly reducing coatings' infection from joint pathogens without affecting the specimens' cytocompatibility. Moreover, copper introduced pro-angiogenic properties as well as it did not affect BG pro-osteogenic activity in vitro. All these findings taken together make the zein/CuBG coating a very promising system to improve the antibacterial and pro-osteointegrative properties of bioinert implantable metallic materials.

CRediT authorship contribution statement

Laura Ramos Rivera: Conceptualization, Methodology, Validation, Formal analysis, Investigation, Data curation, Writing - original draft. **Andrea Cochis:** Conceptualization, Methodology, Validation, Formal analysis, Investigation, Data curation, Writing - original draft. **Sarah Biser:** Methodology, Validation, Investigation, Writing - review & editing. **Elena Canciani:** Methodology, Formal analysis, Investigation, Writing - review & editing, Supervision. **Sara Ferraris:** Methodology, Investigation, Resources, Writing - review & editing, Supervision, Funding acquisition. **Lia Rimondini:** Conceptualization, Formal analysis, Resources, Writing - review & editing, Supervision, Project administration, Funding acquisition. **Aldo R. Boccaccini:** Conceptualization, Formal analysis, Resources, Writing - review & editing, Supervision, Project administration, Funding acquisition.

Acknowledgements

Laura Ramos Rivera thanks the German Academic Exchange Service (DAAD) (Germany) for a fellowship and COLCIENCIAS (Colombia) for financial support.

Appendix A. Supplementary data

Supplementary data to this article can be found online at https://doi.org/10.1016/j.bioactmat.2020.11.001.

References

[1] S.B. Goodman, Z. Yao, M. Keeney, F. Yang, The future of biologic coatings for orthopaedic implants, Biomaterials 34 (2013) 3174–3183, https://doi.org/10.1016/j.biomaterials.2013.01.074.
[2] O. Pillai, R. Panchagnula, Polymers in drug delivery, Curr. Opin. Chem. Biol. 5 (2001) 447–451.
[3] L.Y. Qiu, Y.H. Bae, Polymer architecture and drug delivery, Pharm. Res. (N. Y.) 23 (2006) 1–30, https://doi.org/10.1007/s11095-005-9046-2.
[4] L.L. Hench, The story of Bioglass®, J. Mater. Sci. Mater. Med. 17 (2006) 967–978, https://doi.org/10.1007/s10856-006-0432-z.
[5] E. Fiume, J. Barberi, E. Verné, Bioactive glasses: from parent 45S5 composition to scaffold-assisted tissue-healing therapies, J. Funct. Biomater. 9 (2018) 24, https://doi.org/10.3390/jfb9010024.
[6] M. Mehdipour, A. Afshar, M. Mohebali, Electrophoretic deposition of bioactive glass coating on 316L stainless steel and electrochemical behavior study, Appl. Surf. Sci. 258 (2012) 9832–9839, https://doi.org/10.1016/j.apsusc.2012.06.038.
[7] F. Gebhardt, S. Seuss, M.C. Turhan, H. Hornberger, S. Virtanen, A.R. Boccaccini, Characterization of electrophoretic chitosan coatings on stainless steel, Mater. Lett. 66 (2012) 302–304. https://doi.org/10.1016/j.matlet.2011.08.088.
[8] C.L. Romanò, H. Tsuchiya, I. Morelli, A.G. Battaglia, L. Drago, Antibacterial coating of implants: are we missing something? Bone Joint Res. 8 (2019) 199–206, https://doi.org/10.1302/2046-3758.85.BJR-2018-0316.
[9] S.R. Bharathi Devi, M.A. Dhivya, K.N. Sulochana, Copper transporters and chaperones: their function on angiogenesis and cellular signalling, J. Biosci. 41 (2016) 487–496, https://doi.org/10.1007/s12038-016-9629-6.
[10] J. Barralet, U. Gbureck, P. Habibovic, E. Vorndran, C. Gerard, C.J. Doillon, Angiogenesis in calcium phosphate scaffolds by inorganic copper ion release, Tissue Eng. 15 (2009) 1601–1609, https://doi.org/10.1089/ten.tea.2007.0370.
[11] C. Gérard, L.-J. Bordeleau, J. Barralet, C.J. Doillon, The stimulation of angiogenesis and collagen deposition by copper, Biomaterials 31 (2010) 824–831, https://doi.org/10.1016/j.biomaterials.2009.10.009.
[12] J.P. Rodríguez, S. Ríos, M. González, Modulation of the proliferation and differentiation of human mesenchymal stem cells by copper, J. Cell. Biochem. 85 (2002) 92–100, https://doi.org/10.1002/jcb.10111.
[13] M. Vincent, R.E. Duval, P. Hartemann, M. Engels-Deutsch, Contact killing and antimicrobial properties of copper, J. Appl. Microbiol. 124 (2018) 1032–1046, https://doi.org/10.1111/jam.13681.
[14] G. Grass, C. Rensing, M. Solioz, Metallic copper as an antimicrobial surface, Appl. Environ. Microbiol. 77 (2011) 1541–1547, https://doi.org/10.1128/AEM.02766-10.
[15] A. Hoppe, R. Meszaros, C. Stähli, S. Romeis, J. Schmidt, W. Peukert, B. Marelli, S. N. Nazhat, L. Wondraczek, J. Lao, E. Jallot, A.R. Boccaccini, In vitro reactivity of Cu doped 45S5 Bioglass® derived scaffolds for bone tissue engineering, J. Mater. Chem. B. 1 (2013) 5659–5674, https://doi.org/10.1039/C3TB21007C.
[16] A. Bari, N. Bloise, S. Fiorilli, G. Novajra, M. Vallet-Regí, G. Bruni, A. Torres-Pardo, J.M. González-Calbet, L. Visai, C. Vitale-Brovarone, Copper-containing mesoporous bioactive glass nanoparticles as multifunctional agent for bone regeneration, Acta Biomater. 55 (2017) 493–504, https://doi.org/10.1016/j.actbio.2017.04.012.
[17] J. Bejarano, P. Caviedes, H. Palza, Sol–gel synthesis and in vitro bioactivity of copper and zinc-doped silicate bioactive glasses and glass-ceramics, Biomed. Mater. 10 (2015), 025001, https://doi.org/10.1088/1748-6041/10/2/025001.
[18] J.V. Rau, M. Curcio, M.G. Raucci, K. Barbaro, I. Fasolino, R. Teghil, L. Ambrosio, A. De Bonis, A.R. Boccaccini, Cu-Releasing bioactive glass coatings and their in vitro properties, ACS Appl. Mater. Interfaces 11 (2019) 5812–5820, https://doi.org/10.1021/acsami.8b19082.
[19] J.N. Oliver, Y. Su, X. Lu, P.-H. Kuo, J. Du, D. Zhu, Bioactive glass coatings on metallic implants for biomedical applications, Bioact. Mater. 4 (2019) 261–270, https://doi.org/10.1016/j.bioactmat.2019.09.002.
[20] R. Sikkema, K. Baker, I. Zhitomirsky, Electrophoretic deposition of polymers and proteins for biomedical applications, Adv. Colloid Interface Sci. 284 (2020) 102272, https://doi.org/10.1016/j.cis.2020.102272.
[21] R.B. Heimann, Thermal spraying of biomaterials, Surf. Coating. Technol. 201 (2006) 2012–2019, https://doi.org/10.1016/j.surfcoat.2006.04.052.
[22] R.V. Chernozem, M.A. Surmeneva, B. Krause, T. Baumbach, V.P. Ignatov, A. I. Tyurin, K. Loza, M. Epple, R.A. Surmenev, Hybrid biocomposites based on titania nanotubes and a hydroxyapatite coating deposited by RF-magnetron sputtering: surface topography, structure, and mechanical properties, Appl. Surf. Sci. 426 (2017) 229–237, https://doi.org/10.1016/j.apsusc.2017.07.199.
[23] L. Besra, M. Liu, A review on fundamentals and applications of electrophoretic deposition (EPD), Prog. Mater. Sci. (2007), https://doi.org/10.1016/j.pmatsci.2006.07.001.
[24] P. Sarkar, P.S. Nicholson, Electrophoretic Deposition (EPD): Mechanisms, Kinetics, and Application to Ceramics, 2005, https://doi.org/10.1111/j.1151-2916.1996.tb08929.x.
[25] I. Zhitomirsky, Cathodic electrodeposition of ceramic and organoceramic materials. Fundamental aspects, Adv. Colloid Interface Sci. 97 (2002) 279–317.
[26] F. Pishbin, A. Simchi, M.P. Ryan, A.R. Boccaccini, Electrophoretic deposition of chitosan/45S5 Bioglass® composite coatings for orthopaedic applications, Surf. Coating. Technol. 205 (2011) 5260–5268, https://doi.org/10.1016/j.surfcoat.2011.05.026.
[27] Q. Chen, L. Cordero-Arias, J.A. Roether, S. Cabanas-Polo, S. Virtanen, A. R. Boccaccini, Alginate/Bioglass® composite coatings on stainless steel deposited by direct current and alternating current electrophoretic deposition, Surf. Coating. Technol. 233 (2013) 49–56, https://doi.org/10.1016/j.surfcoat.2013.01.042.
[28] N. Mayer, L.R. Rivera, T. Ellis, J. Qi, M.P. Ryan, A.R. Boccaccini, Bioactive and antibacterial coatings based on zein/bioactive glass composites by electrophoretic deposition, Coatings 8 (2018) 27, https://doi.org/10.3390/coatings8010027.
[29] R. Shukla, M. Cheryan, Zein: the industrial protein from corn, Ind. Crop. Prod. 13 (2001) 171–192, https://doi.org/10.1016/S0926-6690(00)00064-9.
[30] Y. Zhang, L. Cui, X. Che, H. Zhang, N. Shi, C. Li, Y. Chen, W. Kong, Zein-based films and their usage for controlled delivery: origin, classes and current landscape, J. Contr. Release 206 (2015) 206–219, https://doi.org/10.1016/j.jconrel.2015.03.030.
[31] J.J. Harrison, C.A. Stremick, R.J. Turner, N.D. Allan, M.E. Olson, H. Ceri, Microtiter susceptibility testing of microbes growing on peg lids: a miniaturized biofilm

model for highthroughput screening, Nat. Protoc. 5 (2010) 1236–1254, https://doi.org/10.1038/nprot.2010.71.
[32] A. Cochis, J. Barberi, S. Ferraris, M. Miola, L. Rimondini, E. Vernè, S. Yamaguchi, S. Spriano, Competitive surface colonization of antibacterial and bioactive materials doped with strontium and/or silver ions, Nanomaterials 10 (2020) 120, https://doi.org/10.3390/nano10010120.
[33] S. Ferraris, A. Cochis, M. Cazzola, M. Tortello, A. Scalia, S. Spriano, L. Rimondini, Cytocompatible and anti-bacterial adhesion nanotextured titanium oxide layer on titanium surfaces for dental and orthopedic implants, Front. Bioeng. Biotechnol. 7 (2019), https://doi.org/10.3389/fbioe.2019.00103.
[34] H. Obokota, M. Yamato, S. Tsuneda, T. Okano, Reproducible subcutaneous transplantation of cell sheets into recipient mice, Nat. Protoc. 6 (2011) 1053–1059, https://doi.org/10.1038/nprot.2011.356.
[35] Z. Zhang, X. Cheng, Y. Yao, J. Luo, Q. Tang, H. Wu, S. Lin, C. Han, Q. Wei, L. Chen, Electrophoretic deposition of chitosan/gelatin coatings with controlled porous surface topography to enhance initial osteoblast adhesive responses, J. Mater. Chem. B. 4 (2016) 7584–7595, https://doi.org/10.1039/C6TB02122K.
[36] Y.-C. Yin, S.-W. Yin, X.-Q. Yang, C.-H. Tang, S.-H. Wen, Z. Chen, B. Xiao, L.-Y. Wu, Surface modification of sodium caseinate films by Zein coatings, Food Hydrocolloids 36 (2014) 1–8, https://doi.org/10.1016/j.foodhyd.2013.08.027.
[37] T. Lin, C. Lu, L. Zhu, T. Lu, The biodegradation of zein in vitro and in vivo and its application in implants, AAPS PharmSciTech 12 (2011) 172–176, https://doi.org/10.1208/s12249-010-9565-y.
[38] L.L. Hench, H.A. Paschall, Direct chemical bond of bioactive glass-ceramic materials to bone and muscle, J. Biomed. Mater. Res. 7 (1973) 25–42, https://doi.org/10.1002/jbm.820070304.
[39] H. Xie, Y.J. Kang, Role of copper in angiogenesis and its medicinal implications, Curr. Med. Chem. 16 (2009) 1304–1314.
[40] C.K. Sen, S. Khanna, M. Venojarvi, P. Trikha, E.C. Ellison, T.K. Hunt, S. Roy, Copper-induced vascular endothelial growth factor expression and wound healing, Am. J. Physiol. Cell Physiol. 282 (2002) H1821–H1827, https://doi.org/10.1152/ajpheart.01015.2001.
[41] K. Karlin, Metalloenzymes, structural motifs, and inorganic models, Science 261 (1993) 701–708, https://doi.org/10.1126/science.7688141.
[42] Y. Yoshida, S. Furuta, E. Niki, Effects of metal chelating agents on the oxidation of lipids induced by copper and iron, Biochim. Biophys. Acta Lipids Lipid. Metabol. 1210 (1993) 81–88, https://doi.org/10.1016/0005-2760(93)90052-B.
[43] P.J. Newby, R. El-Gendy, J. Kirkham, X.B. Yang, I.D. Thompson, A.R. Boccaccini, Ag-doped 45S5 Bioglass®-based bone scaffolds by molten salt ion exchange: processing and characterisation, J. Mater. Sci. Mater. Med. 22 (2011) 557–569, https://doi.org/10.1007/s10856-011-4240-8.
[44] L.L. Hench, J.M. Polak, Third-generation biomedical materials, Science (80-) (2002) 295, https://doi.org/10.1126/science.1067404, 1014 LP – 1017.
[45] E. Vernè, S. Ferraris, C. Vitale-Brovarone, A. Cochis, L. Rimondini, Bioactive glass functionalised with alkaline phosphatase stimulates bone extracellular matrix deposition and calcification in vitro, Appl. Surf. Sci. 313 (2014) 372–381, https://doi.org/10.1016/j.apsusc.2014.06.001.
[46] C. Stähli, M. James-Bhasin, A. Hoppe, A.R. Boccaccini, S.N. Nazhat, Effect of ion release from Cu-doped 45S5 Bioglass® on 3D endothelial cell morphogenesis, Acta Biomater. 19 (2015) 15–22, https://doi.org/10.1016/j.actbio.2015.03.009.
[47] H. Xie, P. Wang, J. Wu, Effect of exposure of osteoblast-like cells to low-dose silver nanoparticles: uptake, retention and osteogenic activity, Artif. Cells, Nanomedicine, Biotechnol. 47 (2019) 260–267, https://doi.org/10.1080/21691401.2018.1552594.
[48] D. Baldoni, U. Furustrand Tafin, S. Aeppli, E. Angevaare, A. Oliva, M. Haschke, W. Zimmerli, A. Trampuz, Activity of dalbavancin, alone and in combination with rifampicin, against meticillin-resistant Staphylococcus aureus in a foreign-body infection model, Int. J. Antimicrob. Agents 42 (2013) 220–225, https://doi.org/10.1016/j.ijantimicag.2013.05.019.
[49] A. Arkudas, A. Balzer, G. Buehrer, I. Arnold, A. Hoppe, R. Detsch, P. Newby, T. Fey, P. Greil, R.E. Horch, A.R. Boccaccini, U. Kneser, Evaluation of angiogenesis of bioactive glass in the arteriovenous loop model, Tissue Eng. C Methods 19 (2013) 479–486, https://doi.org/10.1089/ten.tec.2012.0572.
[50] G. Giavaresi, P. Torricelli, P.M. Fornasari, R. Giardino, R. Barbucci, G. Leone, Blood vessel formation after soft-tissue implantation of hyaluronan-based hydrogel supplemented with copper ions, Biomaterials 26 (2005) 3001–3008, https://doi.org/10.1016/j.biomaterials.2004.08.027.
[51] C. Wu, Y. Zhou, M. Xu, P. Han, L. Chen, J. Chang, Y. Xiao, Copper-containing mesoporous bioactive glass scaffolds with multifunctional properties of angiogenesis capacity, osteostimulation and antibacterial activity, Biomaterials 34 (2013) 422–433, https://doi.org/10.1016/j.biomaterials.2012.09.066.